Available online at www.sciencedirect.com

ScienceDirect

journal homepage: http://www.elsevier.com/locate/acme

Original Research Article

Shear behavior of two-span fiber reinforced concrete beams

Julita Krassowska [a], *Marta Kosior-Kazberuk* [a], *Piotr Berkowski* [b,*]

[a] *Bialystok University of Technology, Faculty of Civil and Environmental Engineering, Wiejska 45E, 15-351 Bialystok, Poland*

[b] *Wroclaw University of Science and Technology, Faculty of Civil Engineering, Wyb. Wyspianskiego 27, Wroclaw, Poland*

ARTICLE INFO

Article history:
Received 10 December 2018
Received in revised form
5 September 2019
Accepted 22 September 2019
Available online 25 October 2019

Keywords:
Two-span beam
Shear behavior
Fiber reinforced concrete
Steel fiber
Basalt fiber

ABSTRACT

The presented study was conducted to assess the shear capacity and the mechanical behavior of fiber reinforced concrete two-span beams in a five-point bending test. Experimental research was focused on observing changes in the behavior of tested elements depending on the amount of shear reinforcement (stirrups) and the fiber type used. The beams had varied stirrup spacing and two sorts of fibers were used as dispersed reinforcement. The steel fiber content was 78.5 kg/m^3 and the basalt fiber content was 5.0 kg/m^3. Concrete beams without addition of fibers were also examined as reference ones. The effectiveness of both sorts of fibers as shear reinforcement was assessed on the basis of strain development and crack pattern analysis. The digital image correlation technique was used to monitor the development of cracks around the central support of beams. It was shown that fibers control the cracking process and deformations in reinforced concrete beams and they can be effectively used as additional or the only shear reinforcement. The results of shear capacity obtained in the experiment were also compared with the shear capacity calculated according to current design approaches. This analysis has shown that fibers enhance the ultimate shear strength of reinforced concrete beams.

1. Introduction

The development of fiber materials and technology makes it necessary to search for their new applications for different construction purposes. Attention should also be drawn to the modern use of Fiber Reinforced Concrete (FRC), which has entailed experience be obtained over more than 50 years [1,2]. There are more and more outstanding recent applications of fiber reinforced concrete in such elements as pavements and wide range of precast pieces [3], footbridges [4], and tunnels [5]. Among the benefits of adding fibers to structural concrete there are the improvements in flexural and tensile performance [6,7]. The fibers can be used to improve the behavior of structure at the ultimate limit state or to improve service conditions at the serviceability limit state. In the ultimate limit state the addition of

* *Corresponding author.*
E-mail addresses: j.krassowska@pb.edu.pl (J. Krassowska), m.kosior@pb.edu.pl (M. Kosior-Kazberuk), piotr.berkowski@pwr.edu.pl (P. Berkowski).

https://doi.org/10.1016/j.acme.2019.09.005
1644-9665/

fibers can partially or completely replace the traditional reinforcement for tensile or shear [8–11]. The behavior of FRC depends on several factors such as: fiber shapes, constituent materials, fiber dosage, and the final distribution and orientation of fibers located in the concrete element [2,12–15].

Various studies on the shear behavior of Steel Fiber Reinforced Concrete (SFRC) have shown that remarkable improvement of shear capacity and considerable reduction, or even total substitution of steel stirrups, may be obtained by considering the application of steel fibers as shear reinforcement [16–18]. Nonetheless, uncertainties still remain in determining and quantifying the resistant mechanisms of FRC under shear stress when optimizing the reinforcement in each structural problem [19,20]. In order to address this task, the mechanisms that are activated in a cracked element may well be identified as follows: tangential stresses in the area of uncracked concrete (the area under compression in the cross-section of the beam), engagement of the aggregates (aggregate interlock or shear friction at the crack), a pin effect of the longitudinal reinforcement (dowel action), an arch effect, and residual tensile stress across cracks [1,21,22]. Due to the mentioned complex mechanisms,the behavior of fiber-reinforced concrete members in shear is still an intensively investigated field of research, and in the last decades several design approaches have been developed [23–25].

The current design approach of *fib* Model Code 2010 [26] is mainly based on the Simplified Modified Compression Field Theory and the "stress field approach" for shear reinforced members [27]. Eurocode 2 [28] shear design for members without shear reinforcement is partially based on an empirical background. The approach for members with shear reinforcement applies the truss analogy. The shear behavior of fiber-reinforced concrete is less known due to additional factors as the effect of steel fibers and particular shear slip and aggregate interlocking behavior along crack surface [29].

Reinforcing fibers of different materials and sizes have been shown to increase the energy absorption capacity of concrete, and in some cases also an increase in strength properties was observed. Fibers interact with the fracture evolution by delaying the formation of microcracks and the process by which the microcracks link to form the macrocracks. Interest in fiber reinforced concrete structures is growing due to their enhanced toughness [21]. Compared to ordinary concrete, steel fiber reinforced concrete has higher flexural strength, and often compression, and shear strength as well as the increased fatigue resistance and impact resistance. Additionally, the use of steel fibers in members under bending ensures an increase in their resistance to cracking counteracts the effect of shrinkage and prevents the fracture failure of concrete [2,6,7].

Despite the remarkable development in steel fiber reinforced concrete, this material is not yet widely used in structural applications, because it is still difficult to theoretically predict the structural behaviour of fiber reinforced concrete members with conventional shear reinforcement. This makes it difficult to disseminate design methods that take into account the presence of dispersed reinforcement in concrete. Moreover, none of the design approaches takes into account the presence of other fibers in the concrete than steel ones.

In addition to steel fibers, other types of fibers have appeared with new properties for which applications are sought. For example, basalt fibers are a new material whose properties are not yet fully researched. The influence of the mechanical properties of basalt fibers on the load-bearing capacity and deformability of concrete members is also not determined. The most important advantage of basalt fibers is their full corrosion resistance [30,31]. In addition, this fiber exhibits high strength and high module performance. According to Sim et al. [32] the fibers have better tensile strength than the E-glass fibers, greater failure strain than the carbon fibers as well as good resistance to chemical attack, impact load and fire. These features, combined with low cost, could make basalt fibers a suitable replacement for steel, glass, and carbon fibers in many applications [14]. Detailed discussion of basalt fibers influence on the fracture mechanics parameters (such as fracture energy, critical stress intensity factor) can be found in [33].

Considering potential applicability of basalt fibers, further experimental studies should be conducted on the use of this type of fibers in concrete for reinforced structures. The recognition of the failure mode of concrete elements with fibers is crucial for the development of design methods that take the presence of dispersed reinforcement in concrete into account. Extensive work on the effectiveness of using fibers as a replacement of stirrups concerned steel fibers [8–11]. However, there are very few works considering other sorts of fibers in this manner [1].

The aim of the research was the qualitative and quantitative analysis of the influence of dispersed reinforcement, in the form of steel or basalt fibers, partially or completely replacing the typical shear reinforcement of the concrete structure element. In the examined model two-span beams, the influence of the quantity and type of dispersed reinforcement on the process of crack formation and propagation as well as the value of transversal ultimate force was analyzed. In addition, in order to verify the values of these forces, comparative calculations of shear resistance of fiber reinforced elements were made using calculation models currently proposed by standards and recommendations. In order to obtain test results, including tests of shear zones at both external and mid-range supports, taking into account different ratio of bending moment to shear force, as well as to reduce the scatter of measurement results, two-span beams were used in the research.

2. Experimental investigation

2.1. *Concrete mix composition and specimen preparation*

Two types of fibers with different strength properties were used. The geometry and properties of fibers are presented in Table 1. The steel fibers were added to concrete at the content of 78.5 kg/m^3, which gave volume fraction 1.0%, and the basalt fibers were added at the content of 5.0 kg/m^3, which gave volume fraction 0.19%. The influence of fibers on concrete properties was referred to the results obtained for the reference concrete without fibers. The content of both types of fibers was determined on the basis of the previous test results conducted on concrete specimens [33] and model reinforced concrete beams [34]. The analysis of the test results [33] showed a significant effect of 0.19% of basalt fibers addition on the fracture toughness of concrete, and further

Table 1 – Properties of fibers used.

Property	Steel fibers	Basalt fibers
Fiber shape	Hooked end	Straight
Length (mm)	50	50
Diameter (mm)	1.00	0.02
Tensile strength (MPa)	900	1680
Elastic modulus (GPa)	200	89
Density (kg/m^3)	7850	2660

increase in the fiber content did not improve the properties of the concrete. The volume fraction of steel fibers 1.0% ensured the significant effect of fibers in concrete on the shear behavior of beams and further increase in fiber content required special treatment to evenly distribute them in concrete mix [34].

Portland cement CEM I 42.5R was used to make concrete for structural elements. The cement content was 300 kg/m^3. The water to cement ratio was equal to 0.5.

The mixture of sand with a grain diameter up to 2 mm and coarse aggregate with a grain diameter up to 8 mm was used. The composition of aggregate was as follows: fraction up to 2 mm - 51%, fraction 2–4 mm - 20% and fraction 4–8 mm - 29%. The fibers were introduced as a replacement of the adequate portion of aggregate by volume. The modified polycarboxylate and phosphonate based super-plasticizer (1% related to cement mass) was used to minimize fiber clumping and enhance fiber dispersion in concrete.

The dry aggregate was mixed with steel or basalt fibers, respectively, followed by cement. The materials were dry mixed for 2 min. before adding water with super-plasticizer. Mixing continued for a further 4 min. The time of mixing was considered sufficient for the proper dispersion of the fibers in the mix without causing a "balling" effect. The specimens were then vibrated in moulds and stored under polyethylene cover for one day. After demoulding, all specimens were cured in water at the temperature of 18 ± 2 °C until they were tested.

The strength properties of concretes with fibers and reference concrete without fibers were determined. The test of compressive strength was carried out in accordance with PN-EN 12390-3 [35] using cubic samples with 100 mm side size. The flexural strength was determined on specimens of size 100 × 100 × 400 mm according to PN-EN 12390-5 [36]. The elastic modulus was determined in accordance with PN-EN 12390-13 [37] and the splitting tensile strength according to PN-EN 12390-6 [38] using cylindrical samples with a diameter of 150 mm and a depth of 300 mm. Each series of testing the material properties consisted of 12 specimens.

2.2. *Experimental research program for two-span beams*

Twenty seven two-span beams were tested in order to identify the different mechanisms contributing to overall shear resistance and to assess the nature of the shear failure process of reinforced concrete beams with dispersed fiber reinforcement. All beams have a total length of 4150 mm and a single span of 2000 mm (support points were placed at a distance of 75 mm from the utmost edges of the beams) and the rectangular cross-section with dimensions 120 × 300 mm. In the research program, the series of beams differing in the spacing of transversal reinforcement were used to ensure

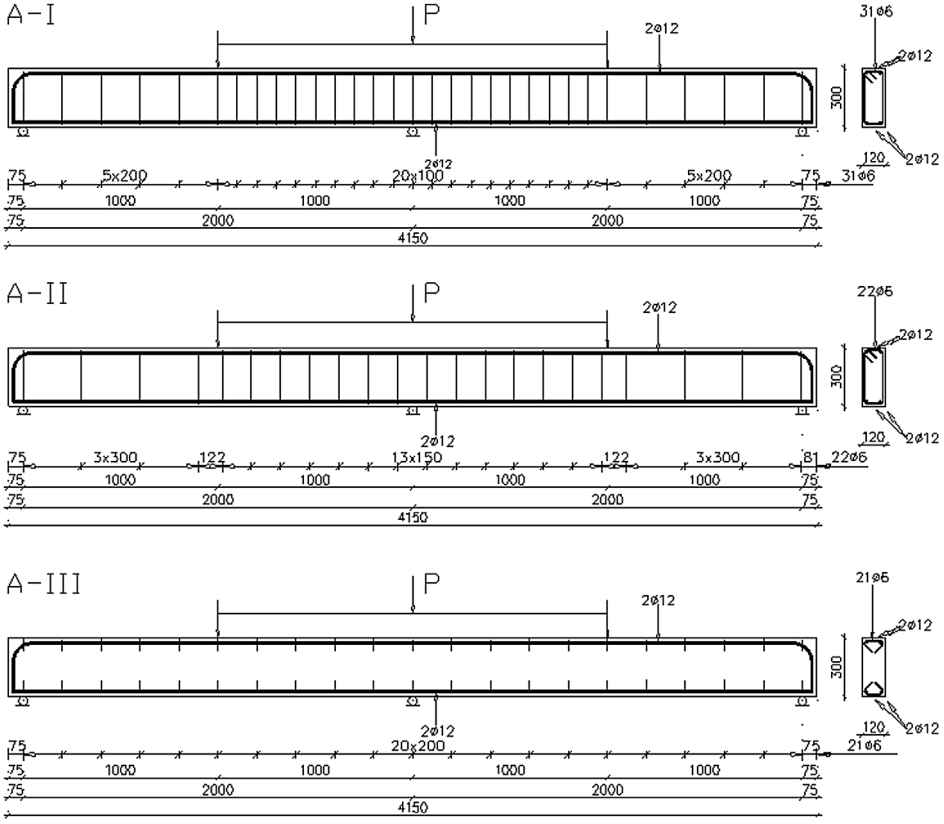

Fig. 1 – Longitudinal and transversal reinforcement in beams tested.

different failure modes. Each series consisted of 3 beams. The geometric dimensions of the test specimens and the schema of reinforcement are shown in Fig. 1.

The amount of main longitudinal reinforcement and shear reinforcement of A-I-0 series were calculated in accordance with Eurocode 2 [28] assuming a load in the form of a concentrated force in the middle of each span (P/2 as in Fig. 1). The degree of longitudinal reinforcement was assumed to be 0.65%, the maximum bending moment and the corresponding shear forces were calculated, on the basis of which the shear reinforcement was determined. The redistribution of forces in the cross-section of beam was assumed in accordance with Eurocode 2 [28]. In each test series, the top and bottom longitudinal reinforcements were identical and consisted of two φ12 mm (f_{yk} = 500 MPa) bars. The concrete cover of longitudinal reinforcement was equal to 15 mm and the length of anchorage of reinforcing ribbed bars l_{bd} was equal to 260 mm. The shear reinforcement calculated for A-I-0 series was reduced by 50% (A-II series) or by total elimination (A-III series). The stirrups with diameter of φ6 mm (f_{yk} = 500 MPa) were used. The ratio of the shear span a_v/d means the ratio of distance from the support to the point of application of the load a_v to the depth of the cross-section d. In case of analysed series the load was applied exactly in the middle of each span of the beam, thus the shear span/effective depth ratio a_v/d was equal to 3.7. Beams were reinforced symmetrically with respect to the central support. The increase in the spacing of stirrups in particular series was aimed at demonstrating the possibility of limiting the number of stirrups, whose task will partially be taken over by the fibers added to the concrete. Series A-I beams were reinforced with shear stirrups spacing calculated according to Eurocode 2 [28]. In A-II series, the stirrups had spacing twice as large as determined according to Eurocode 2 [28]. There were no stirrups in A-III series beams. All the beams were prepared at the prefabrication plant. A description of the beam specimen series is shown in Table 2.

Fig. 2 shows the test stand with equipment used for measurements. The measurement of support reactions was made by means of tensometric load sensors arranged in pairs under extreme supports (2 × 50 kN) and under the central support (2 × 100 kN). The reaction values were recorded using a measurement module connected to sensors. The strains at the top of beams in the concrete compression zone and in the tensile zone at the bottom of the beams were recorded by means of strain gauges installed at the concrete surface in the mid-span of both spans, at the location of top and bottom reinforcement. The development of crack pattern and the width of cracks were also measured using Brinell microscope. However, the manual measurements of cracks may provide only limited information, therefore, a Digital Image Correlation (DIC) technique using a digital recording camera ''Aramis'' by GOM

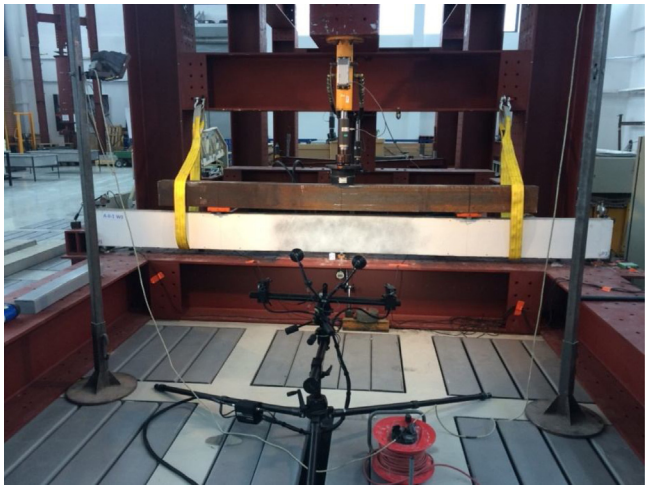

Fig. 2 – Test setup with beam specimen.

(Fig. 2) was applied in addition, to monitor the development of the cracks and measure their widths, and to detect strain components. DIC is an optical, non-contacting measuring technique, enabling to determine the displacement and deformation field of a specimen's surface under any type of loading condition [39,40]. All the data resulting from the tests were recorded automatically using data logger. The DIC-based non-contact measurement system was placed on the side of the beam and the crack pattern around the central support. A uniform/random speckle pattern was applied on the surface of the beam. With system calibration, an area (about 1000 × 300 mm - depth of beam) of view of DIC measurement system can be obtained. In the experiment performed, two cameras were placed in a way enabling to film a total area of 1000 × 300 mm by each camera on either side of the central support.

The beams were loaded in a five-point system using a force increase every 10 kN, until the specimen failed. The load was set using a hydraulic servo with a capacity of 500 kN (HYSDOZOK loading system). The beams have been preloaded to 30 kN. Then, the time of the load increase was 30 s for 10 kN (every step in measurement process), then for 30 s a constant load was kept in order to carry out recording the measured quantities. The values of loads at which the first crack and the first diagonal crack appeared were recorded from the indications of the measuring system performing the test in the next step of the measurement process. The measurement of deflection lasted either until reaching the maximum measuring range of the sensor or the measurement sensor was removed when it was observed that the beam may damage it during destruction (in the last measurement step the sensor

Table 2 – Designation of beam specimens.

Series	Spacing of stirrups [cm]	Reference beams (no fibers)	Beams of concrete with steel fibers (78.5 kg/m^3)	Beams of concrete with basalt fibers (5.0 kg/m^3)
A-I	10/20	A-I-0	A-I-S	A-I-B
A-II	15/30	A-II-0	A-II-S	A-II-B
A-III	no stirrups	A-III-0	A-III-S	A-III-B

Table 3 – Strength properties of concretes (average values and range of accuracy).

Fiber type	V_f [kg/m^3]	f_{cm} [MPa]	f_{ctm} [MPa]	f_{cl} [MPa]	E [GPa]
No fibers	0	52.96 (±6.36)	5.14 (±0.33)	3.22 (±0.39)	33.29 (±1.28)
steel	78.5 (1.0%)	52.05 (±6.18)	7.21 (±1.06)	5.45 (±0.51)	33.71 (±0.34)
basalt	5.00 (0.19%)	46.24 (±5.35)	6.72 (±1.22)	4.49 (±0.24)	32.86 (±2.33)

was removed from the test field under the beam), or the last measurement result was omitted from the graph (after the beam has already broken), because it could interfere with the entire deflection function.

3. Analysis of test results

3.1. *Properties of concretes*

The test results of concrete strength properties: compressive strength f_{cm}, flexural strength f_{ctm}, splitting tensile strength f_{cl}, and modulus of elasticity E in relation to the fiber types in concrete (V_f) are presented in Table 3.

The presence of fibers has no significant influence on the average compressive strength f_{cm} of steel fiber reinforced concrete (Table 3) in comparison to the reference concrete while the concrete with basalt fibers was characterized by compressive strength lower by 10% in comparison to the reference one. The increase in flexural strength f_{ctm} of concrete with steel fibers and concrete with basalt fibers in comparison to the reference concrete was 40% and 30%, respectively. The increase in splitting tensile strength f_{cl} was as high as 69% for concrete with steel fibers and 40% for concrete with basalt fibers in comparison to reference one. The incorporation of fibers into concrete caused the increase in both the ultimate load and the ductility. Any of the fiber types used had no influence on the modulus of elasticity E.

3.2. *Ultimate load*

Table 4 shows the average values of ultimate load P_{ult} for beams made of concrete with fibers and their increase ΔP_{ult} in comparison to the values of destructive loads recorded for the reference beams (without fibers). The values of the ultimate forces shown in Table 4 refer to the maximum force at which their failure occurred. The A-I series beams were assumed as reference ones due to the fact that they were designed according to the EC2 guidelines. Comparing the ultimate force values obtained in the tests for the remaining series of beams to the forces defined for the A-I series beams is meant to show the change in the value of the maximum load depending on the used beam reinforcement model.

For all the A-I series beams failure occurred due to the flexural tension. The significant deformations due to bending were observed in the case of the A-II series beams, however they have eventually failed due to shear. All A-III series beams without stirrups failed due to shear. The influence of the dispersed reinforcement on the shear capacity can be assessed by comparing the value of ultimate load in individual series. In the case of A-I beam series the value of ultimate force increased slightly for concrete beams with basalt or steel fibers. Greater increase in P_{ult}, caused by incorporation of both types of fibers in concrete, was observed in series A-II (19% and 31% respectively, for basalt fibers and steel fibers). In the A-II-B series the value of ultimate force was comparable to the value of the force recorded for the A-I-0 series. It can be concluded that the incorporation of basalt fibers caused an increase in the ultimate force, despite the use of only half number of stirrups. The average ultimate force in the A-II-S series (concrete with steel fibers) was considerably greater than the average force in the A-I-0 series.

The beams of A-III series were not reinforced with stirrups, and the role of stirrups was taken over by the dispersed reinforcement. In this case the effect of fiber reinforcement on beam capacity was the most significant. In beams made of concrete with basalt fibers the ultimate force increased by 23%, compared to reference concrete beams. By using concrete with steel fibers, an increase in the ultimate force of two-span beam was achieved by as much as 87%. Comparing the ultimate loads for beams of the A-III series made of concrete with fibers with the ultimate force recorded for A-I-0 series, only 8% decrease in ultimate load for A-III-S series and as much as 40% decrease in the case of A-III-B were observed. The bridging effect of steel fibers during the failure of beam was more effective compared to basalt fibers. The rigid steel fibers were drawn out from the cement matrix, while the thin basalt fibers were broken.

3.3. *Load-deflection characteristics*

Figs. 3–5 present the load P versus mid-span deflection a curves for beams tested. The mid-span deflections recorded at the centre of both spans of beams were averaged. The load-deflection

Table 4 – Ultimate load P_{ult} and their increase ΔP_{ult} in particular series in comparison to series without fibers (average values and range of accuracy).

Fiber type	No fiber (0)	Basalt fibers (B)		Steel fibers (S)	
Series	P_{ult} [kN]	P_{ult} [kN]	ΔP_{ult} [%]	P_{ult} [kN]	ΔP_{ult} [%]
A-I	222 (±20)	229 (±8)	3	258 (±6)	16
A-II	193 (±4)	228 (±8)	19	252 (±6)	31
A-III	109 (±20)	134 (±21)	23	204 (±14)	87

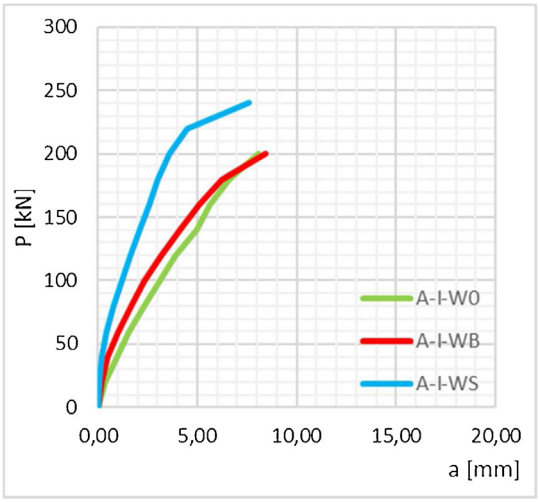

Fig. 3 – Load *P* vs. mid-span deflection *a* for A-I series beams.

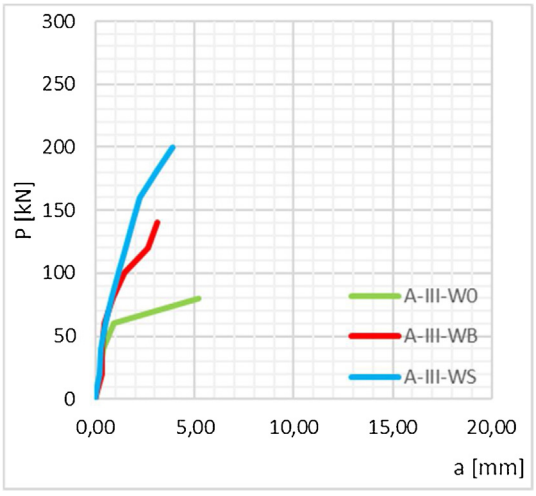

Fig. 5 – Load *P* vs. mid-span deflection *a* for A-III series beams.

dependencies presented in Figs. 3–5 have been developed on the basis of average values of measurements taken for three beams, including settlement of supports.

In all series the deflections of beams made of concrete with dispersed reinforcement at the same level of load were smaller than in the reference concrete beams. The addition of basalt fiber to concrete resulted in a slight reduction of the deflection as compared to reference concrete members in the A-I series, while the incorporation of steel fibers into concrete caused the reduction of deflection by as much as a half for the same level of load. For A-II-WB and A-II-WS series the deflections of beams lower by approx. 30–50% in comparison to A-II-0 series were observed. For the A-III series, with only longitudinal reinforcement without shear reinforcement, in the case of concrete beams with steel fibers, the maximum value of deflection was reduced by 30%, and in the case of using concrete with basalt fiber this value decreased by 20% in relation to reference beams.

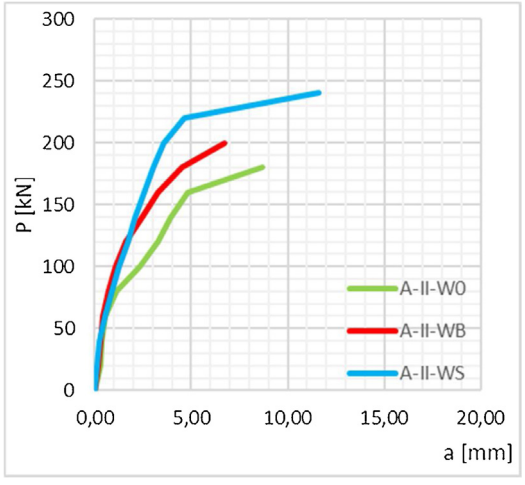

Fig. 4 – Load *P* vs. mid-span deflection *a* for A-II series beams.

The comparison of curves in Figs. 3–5 shows that the addition of fiber (steel or basalt) reinforcement in an adequate percentage can modify the failure mode. The ductile flexural mode was revealed by the increase in the ultimate load value and the post-peak curve, which for beam series with steel fibers (A-I-S and A-II-S) became almost linear forming a plateau. In the case of beams of concrete with basalt fibers nonlinear relationship with gradual reducing slope was observed up to failure. Both sorts of fibers used provided significant performance at serviceability limit state by improving the tension-stiffening effect and, therefore reducing the deflection. However, the steel fibers in considered amount in concrete were more effective. They caused the elongation of linear part of curve, the increase in the ultimate load value and significant changes of post-peak performance. The plateau could be observed in the load-deflection plot after reaching the maximum load in the case of concrete beams with steel fibers (Figs. 3 and 4). The effect of basalt fibers on the reduction of deflection was particularly evident in the case of the A-II-B and A-III-B series.

3.4. *Crack patterns in beams*

The analysis of crack pattern (Figs. 6–8) shows how the incorporation of fibers in concrete influences the failure mode of beams with the same transverse reinforcement.

The development of cracking of selected A-I series beams is shown in Fig. 6. As it was expected, their failure occurred due to the flexural tension. The cracks perpendicular to the longitudinal axis appeared as the first ones in the center of the span of the reference beams (A-I-0) at a load level of 0.3 P_{ult}, whereas in fiber-reinforced concrete beams the first cracks appeared at a load of 0.4 P_{ult}. As the load increased, further cracks appeared in the central part of the spans, and they propagated to a depth of 200 mm from the bottom edge of the beam. In the case of reference beams (A-I-0) and basalt fiber reinforced concrete beams (A-I-B), there were also cracks at the central support at the level load of 0.4 P_{ult}, while in case of steel fiber reinforced concrete beams (A-I-S) the first cracks at the

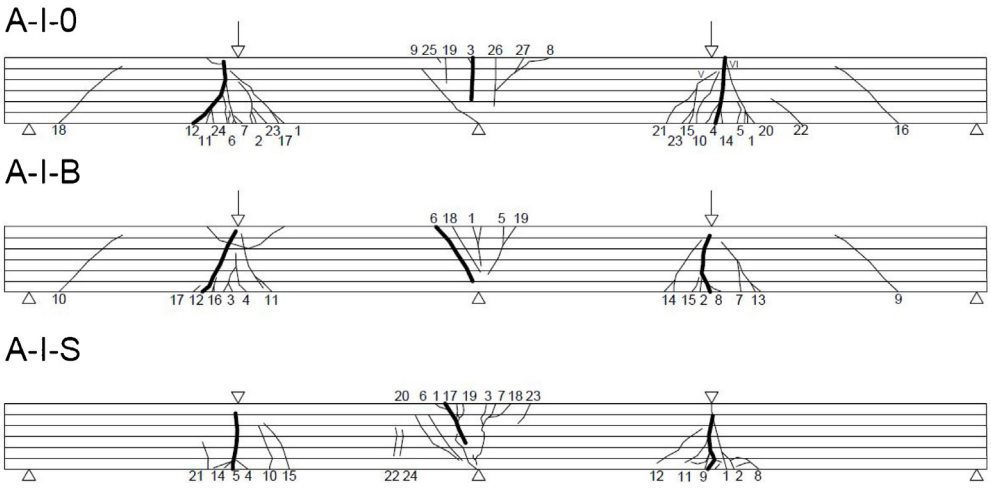

Fig. 6 – Crack pattern in A-I series beams (destructive crack was marked with a thick line).

central support appeared at a load level approx. 15% higher, and achieved the length of 200 mm from the top edge of the beam. The slow and stable development of perpendicular cracks was observed in all beams. Shear cracks appeared at the central support at load level equal to 0.7 P_{ult} for A-I-0 series, and a load level equal to 0.8 P_{ult} for A-I-B series. In the case of beams made of steel fiber reinforced concrete, there were no diagonal cracks at all. The failure of reference concrete beams and basalt fiber reinforced concrete beams occurred due to flexural tension in the middle of the spans and on the central support. The course of the final phase of failure was rather sudden and had a brittle character with a characteristic crack sound. The behavior similar to the behavior of plastic body was observed in the case of A-I-S series, and with the increase in load, the width of already existing cracks increased, with no new ones appearing. The destruction process was slow. In beam series with shear cracks, their propagation ran towards the point of concentrated load application and towards the level of longitudinal reinforcement, and then along the longitudinal reinforcement towards the support.

In the series A-II there were significant differences in the mode of loss of bearing capacity for individual test members (Fig. 7). In the case of A-II-0 and A-II-B series, two plastic hinges were observed, firstly in the middle of the spans, and then the failure process took place mainly by shearing at the central support. The destruction process proceeded violently. Perpendicular cracks (at the load level of approx. 0.35 P_{ult}) and longitudinal ones on the upper surface of beams appeared. The straightening of the stirrup hooks (during the destruction phase) and separation of the lateral and bottom cover of reinforcement were observed. In the case of A-II-S beams, three plastic hinges occurred, first one over the central support (0.8 P_{ult}), and then two hinges in the middle of spans (0.9 P_{ult}). The failure process proceeded in a soft manner, and the significant increases in the deflections of the beams' spans at a constant load were observed.

All beams of A-III series failed due to shear (Fig. 8). The mechanism of crack formation in A-III-0 and in A-III-B series beams was similar. The first cracks appeared at the central support (0.4 P_{ult}), and then the shear failure of element occurred violently. The beams failed in the zero moment cross-section and

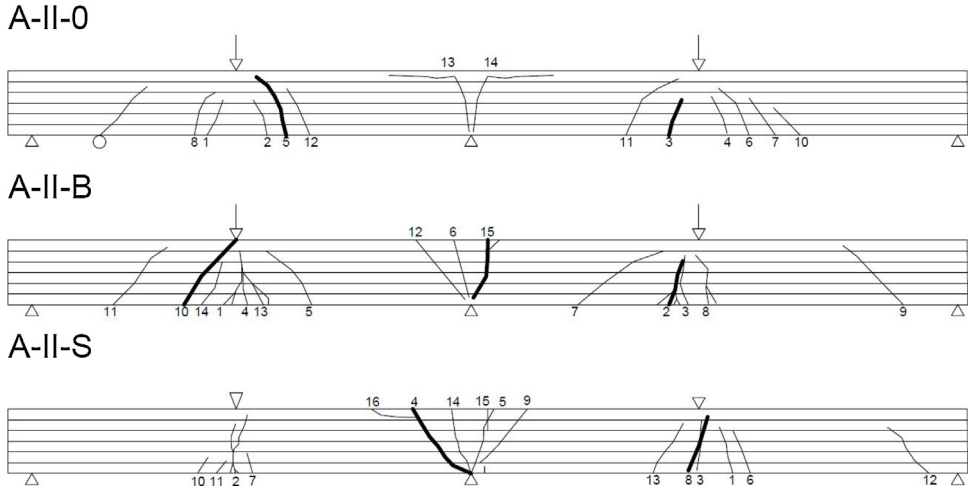

Fig. 7 – Crack pattern in A-II series beams (destructive crack was marked with a thick line).

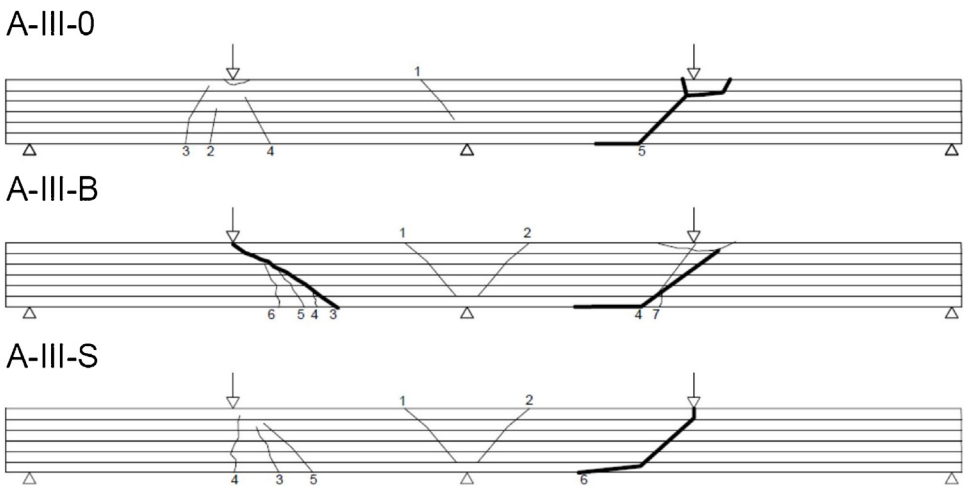

Fig. 8 – Crack pattern in A-III series beams (destructive crack was marked with a thick line).

for the highest shear force (approx. 0.3 l from the central support). The destructive cracks width reached 34 mm. In the A-III-S series elements, the first cracks appeared in the spans at a load level of 0.3 P_{ult}, followed by a stable development of cracks perpendicular to the member axis up to 0.8 of the beam depth. At the load level of 0.8 P_{ult}, a diagonal crack appeared, causing damage. The incorporation of fibers in concrete caused an increase in the value of load initiating the diagonal crack formation about 15% and 30% for basalt fibers and steel fibers, respectively.

Crack patterns for concrete beams of A-III series with fibers and without fibers were significantly different. The reference beams exhibited a single inclined crack and their failure occurred due to the brittle shear, while at least two diagonal cracks (overlapping during failure) appeared in beams made of concrete with fibers. An increase in the number of cracks in beams of concrete with fibers is noticeable, however, they appeared at a higher load than in the reference beams, and were characterized by a smaller width.

A comparison of the average values of the loads causing the first crack perpendicular to the axis of the concrete member and the first diagonal crack loads together with the maximum widths of these cracks were presented in Table 5.

The main strain distribution and crack pattern around the central support of beam were recorded using the Aramis GOM optical data acquisition system. Figs. 9–11 show the strain images around the beam support at the peak load P_{ult}. The analysis of test results allows to assessing the effect of changes in stirrup spacing on the failure mode of beams made of concrete with fibers in comparison to reference beams.

The lighter areas in the images of strain fields indicate the deep range of the tensile zone in concrete caused by intensive cracking of beams just before failure. In the A-I-0 and A-II-0 series, high tensile stresses along the top reinforcement can be observed, related to the gradual loss of adhesion of the longitudinal reinforcement to the concrete. The effect caused by the slip of reinforcement and the loosening of the concrete cover can be seen in Fig. 9a and b. During the failure, the cracks in the beams made of concrete with steel fibers had a much larger width, and their number was smaller compared to reference beams and beams of concrete with basalt fibers. In A-II-B and A-II-S series beams, in contrast to the A-II-0 series beams of reference concrete, there was no local loss of adhesion between the longitudinal reinforcement and concrete. That was the result of the presence of basalt or steel fibers that were able to carry the tensile stresses. Fewer cracks in steel fiber reinforced concrete beams resulted from the greater modulus of elasticity of these fibers, compared to basalt fibers and more effective operation of steel fibers in crack bridging. In the A-III series without the shear reinforcement, the deformations in the support zone were small, which can be compared with a crack pattern diagram of these beams (Fig. 8).

Table 5 – Perpendicular crack load and diagonal crack load (average values and range of accuracy).

Series	First crack load [kN]	Main crack width [mm]	Diagonal crack load [kN]	Main shear crack width [mm]
A-I-0	77 (±4.7)	4.87 (±1.03)	118 (±9.6)	1.58 (±0.38)
A-I-B	90 (±16.3)	3.89 (±0.09)	160 (±7.0)	1.86 (±0.41)
A-I-S	95 (±9.4)	14.20 (±2.38)	220 (±16.3)	0.15 (±0.01)
A-II-0	67 (±9.5)	1.90 (±0.60)	100 (±8.2)	0.50 (±0.04)
A-II-B	73 (±9.0)	4.24 (±0.79)	118 (±12.5)	0.76 (±0.14)
A-II-S	85 (±10.0)	7.84 (±0.84)	136 (±3.5)	1.40 (±0.16)
A-III-0	70 (±9.5)	1.05 (±0.40)	88 (±2.6)	30.16 (±3.37)
A-III-B	86 (±15.2)	2.03 (±0.06)	92 (±9.0)	28.48 (±2.43)
A-III-S	80 (±17.3)	4.03 (±1.21)	123 (±14.2)	23.69 (±4.94)

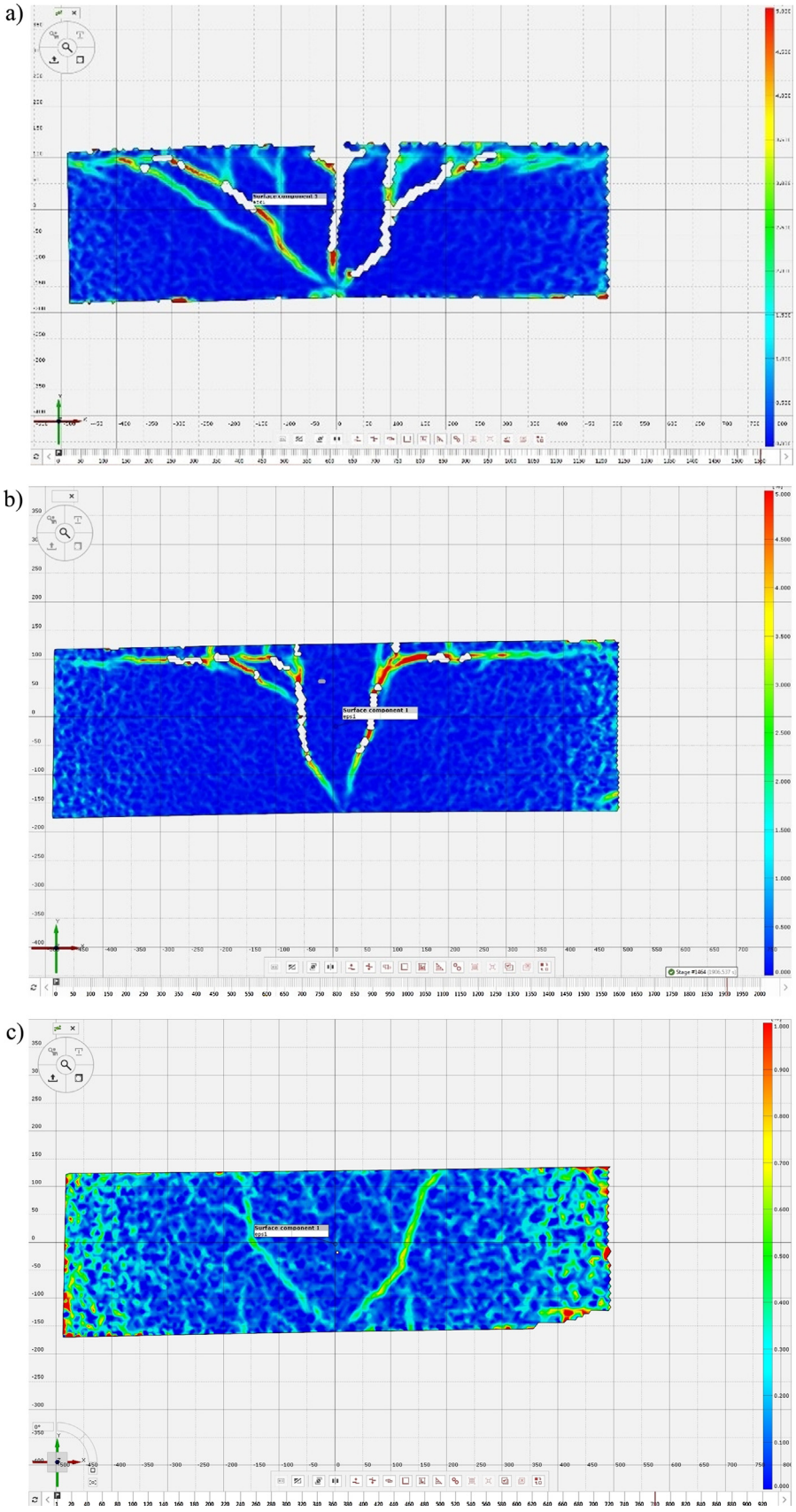

Fig. 9 – Images of strain fields in concrete and crack pattern in beam around the central support at the peak load P_{ult}: (a) A-I-0; (b) A-II-0; (c) A-III-0.

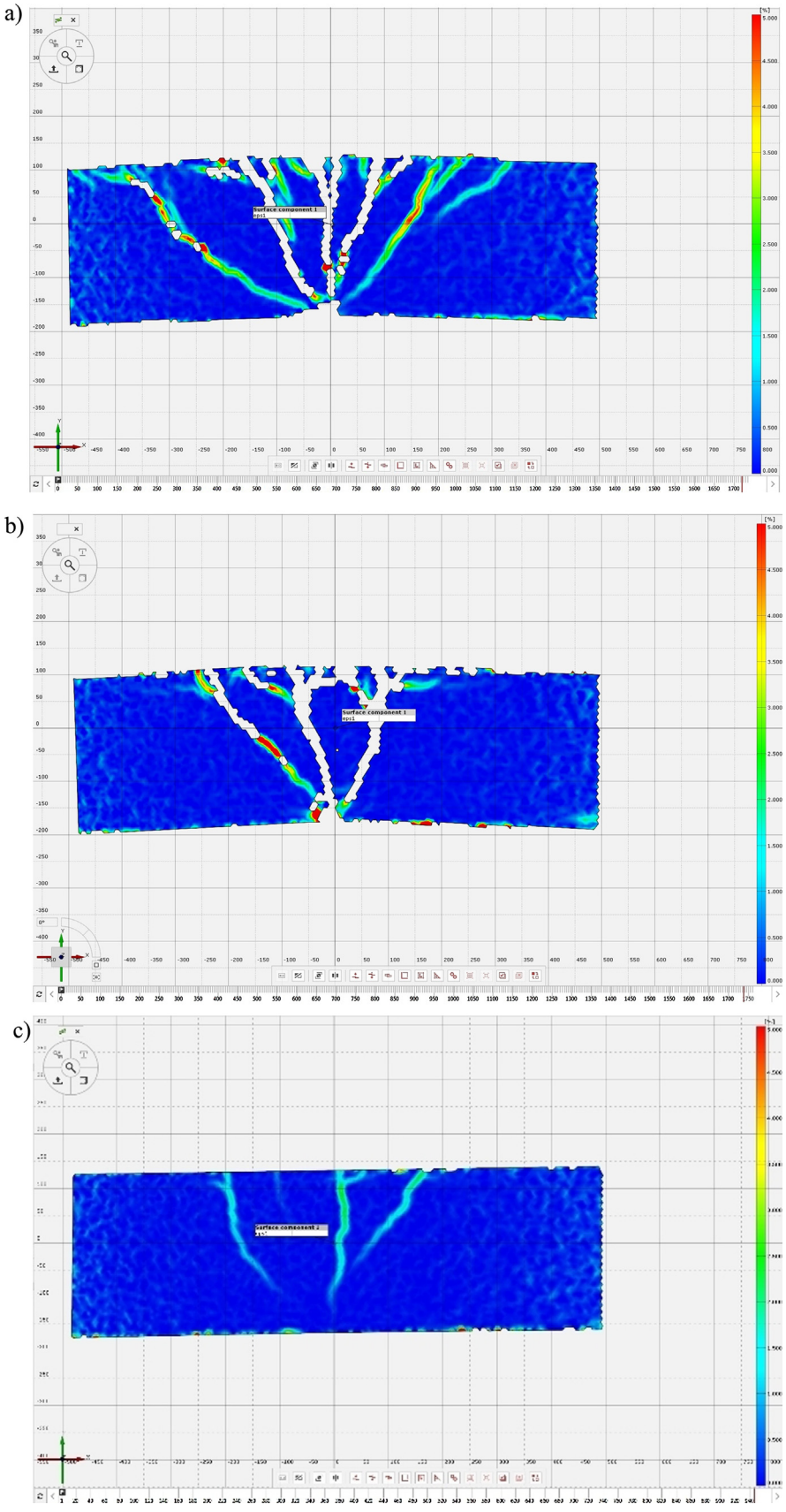

Fig. 10 – Images of strain fields in concrete and crack pattern in beam around the central support at the peak load P_{ult}: (a) A-I-B; (b) A-II-B; (c) A-III-B.

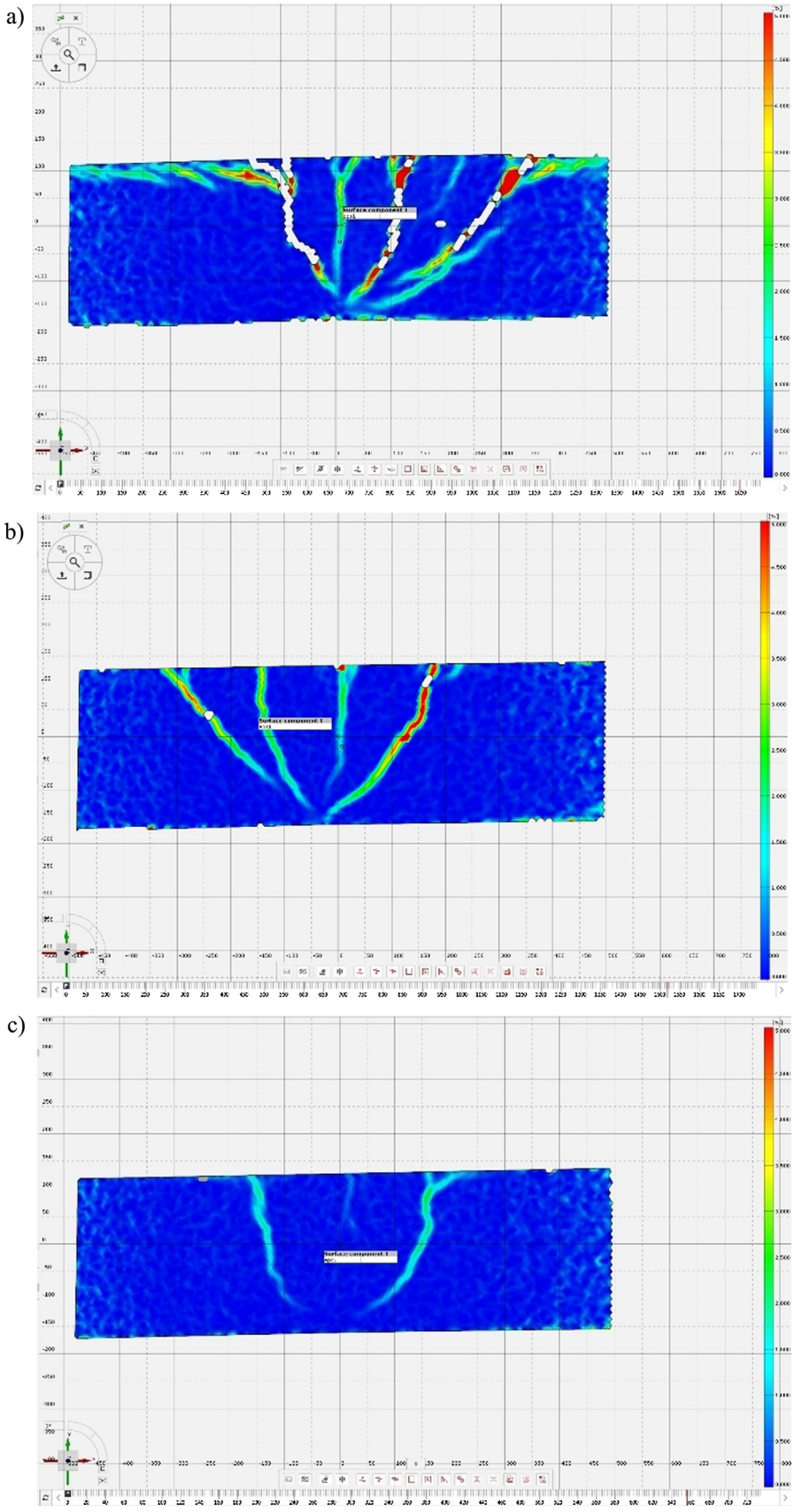

Fig. 11 – Images of strain fields in concrete and crack pattern in beam around the central support at the peak load P_{ult}: (a) A-I-S; (b) A-II-S; (c) A-III-S.

Detailed analysis of the crack pattern in the support zone allows us to approach the explanation of the role of fibers in increasing the shear capacity. All A-I beams have been damaged due to bending. In the support zone, it was possible to observe cracks perpendicular to the axis of the element caused by bending (Figs. 9a, 10a and 11a). In the case of beams reinforced with stirrups (concrete without fibers), the stiffness distribution is similar to the orthotropic material (the stirrups' location determines the direction of deformations because steel stirrups cause the local increase in stiffness). The operation of stirrups and fibers contributed to the increase in shear capacity in a continual way. As a result of reducing the number of stirrups in series A-II, a complex state of stress occurred, resulting in destruction due to flexural tension and shear. Beams with only longitudinal reinforcement (A-III series) failed due to shear. In fiber reinforced concrete beams, a qualitatively different image of maximum strains was observed (comparison of Fig. 9b versus 10b and 11b). Due to the presence of randomly distributed fibers, the concrete behavior becomes similar to that of an isotropic material. Hence, the similarity of the crack pattern in concrete with fibers occurs, e.g. beam reinforced with stirrups of A-II-S series (Fig. 11b) and without fibers, e.g., A-III-0 (no stirrups) in Fig. 9c.

4. Comparison of calculated and experimental values of shear capacity of steel and basalt fiber reinforced concrete beams

The results of measurements of the maximum shear forces V_{Exp} were compared with values of shear capacity in cross-sections near support zones, calculated on the basis of selected procedures according to the *fib* Model Code 2010 [26]. The average values of reactions measured for particular beam series were presented in Figs. 12–20. The calculated values of shear resistance were given in the same figures, independently of the failure mode of beam series. Although the A-I series beams failed due to bending, Figs. 12–14 were presented to show the design bearing capacity of beams with full shear reinforcement, in order to compare their shear resistance with resistance of beams with number of stirrups reduced to half or with beams without stirrups. Thanks to this, a set of calculations of shear resistance of beams considered in the article was included and the differences in approach to shear resistance of beams made of concrete with and without fibers were presented.

In recommendations of the standard [26] for the dimensioning of concrete members for shear, three levels of calculation approximation are distinguished, differing in the completeness of the applied method and the accuracy of the obtained results. In this research work, the level III approximation (V_{MCIII}) was used to calculate the shear capacity of beams of concrete without fibers. The level III approximation is used to design elements in a complex state of stress, regardless of the amount of transversal reinforcement. The theoretical basis for shear dimensioning according to [26] the III level of approximation is the Simplified Modified Compression Field Theory (SMCFT), described inter alia in [23]. At the III level of approximation, the contribution of concrete in the transmission of lateral force resulting from the phenomenon of the aggregate interlock is taken into account.

The level III approximation corresponds to the general form of the formulas for the shear capacity calculation and it is based on the simplified method of compressive stress field

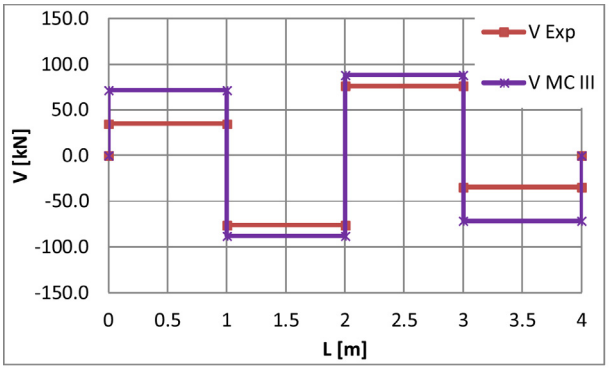

Fig. 12 – Comparison of the shear force value determined experimentally V_{Exp} with the shear capacity calculated on the III level of approximation V_{MCIII} - series A-I-0 (concrete without fibers).

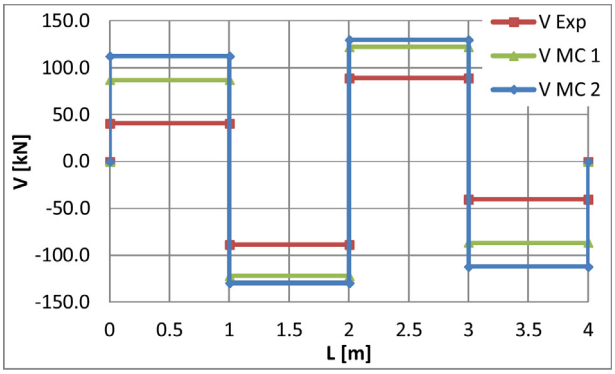

Fig. 13 – Comparison of the shear force value determined experimentally V_{Exp} with the shear capacity calculated according to truss methodV_{MC1} and according to SMCFT V_{MC2} - series A-I-S (concrete with steel fibers).

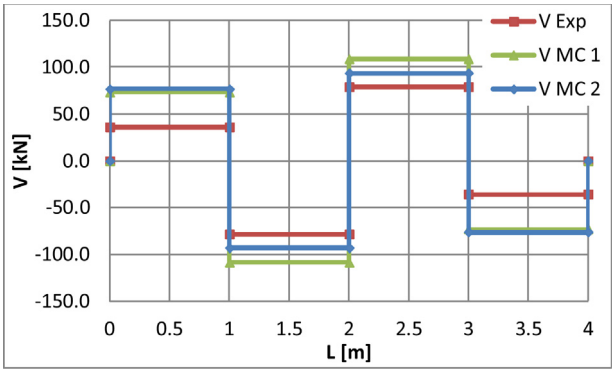

Fig. 14 – Comparison of the shear force value determined experimentally V_{Exp} with the shear capacity calculated according to truss method V_{MC1} and according to SMCFT V_{MC2} - series A-I-B (concrete with basalt fibers).

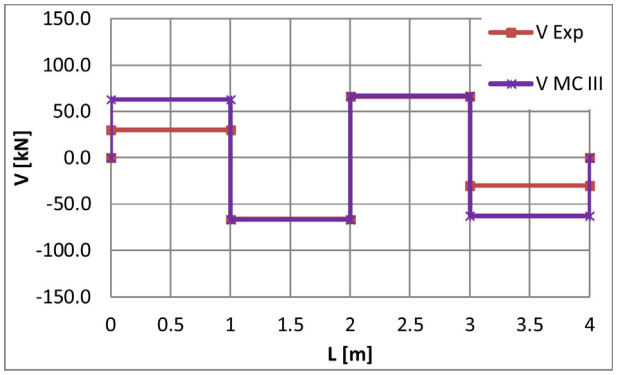

Fig. 15 – Comparison of the shear force value determined experimentally V_{Exp} with the shear capacity calculated on the III level of approximation V_{MCIII} - series A-II-0 (concrete without fibers).

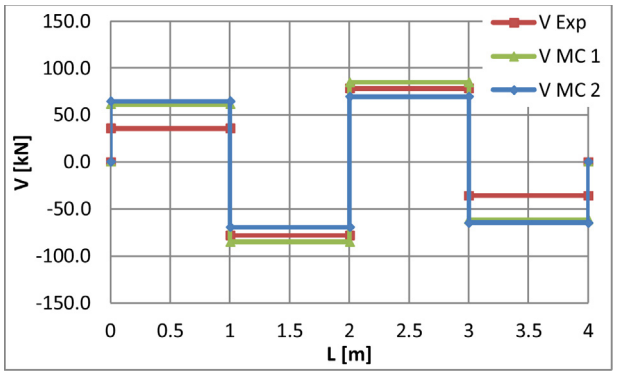

Fig. 17 – Comparison of the shear force value determined experimentally V_{Exp} with the shear capacity calculated according to truss method V_{MC1} and according to SMCFT V_{MC2} - series A-II-B (concrete with basalt fibers).

theory. According to the approach at level III, the design shear resistance V_{Rd}, if $V_{Rd} \le V_{Rd,max}$ (θ_{min}) is defined as follows:

$$V_{Rd} = V_{Rd,c} + V_{Rd,s}. \quad (1)$$

The component of the design shear resistance attributed to the concrete $V_{Rd,c}$ is determined on the basis of formula:

$$V_{Rd,c} = k \cdot \frac{\sqrt{f_{ck}}}{\gamma_c} \cdot b_w \cdot z, \quad (2)$$

where: k_v- coefficient determining the concrete share in shear resistance; f_{ck} - characteristic value of compressive strength on the basis of test results; γ_c - partial safety factor for concrete without fibres; b_w - the smallest width of the cross-section in the tensile area; z - internal lever arm.

The component of the design shear resistance provided by shear reinforcement $V_{Rd,s}$ is determined on the basis of formula:

$$V_{Rd,s} = \frac{A_{sw}}{s_w} \cdot z \cdot f_{ywd} \cdot \cot\theta, \quad (3)$$

where: A_{sw} - area of shear reinforcement; s_w - distance between stirrups; f_{ywd} - yield strength of reinforcing steel; θ - angle denoting the inclination of compressive stress field.

The standard design methods for shear capacity [26] relate to concrete with steel fibers. The proposed procedures have not yet been checked for fibers of other materials and for concrete different from ordinary one. Therefore, in the present research work, the approaches that use the residual tensile strength for bending f_{Ftu} are adopted to estimate the effect of basalt fibers on the shear capacity of beams. In order to estimate the shear resistance of concrete beams with steel and basalt fibers, two approaches were used: the truss method (V_{MC1}) and the Simplified Modified Compression Field Theory - SMCFT (V_{MC2}). For the above approaches, the following definitions have been adopted:

$V_{MC\ 1}$ – the shear capacity of the fiber concrete member calculated on the basis of the *fib* Model Code 2010 procedure [26] based on the truss method, where the influence of fibers

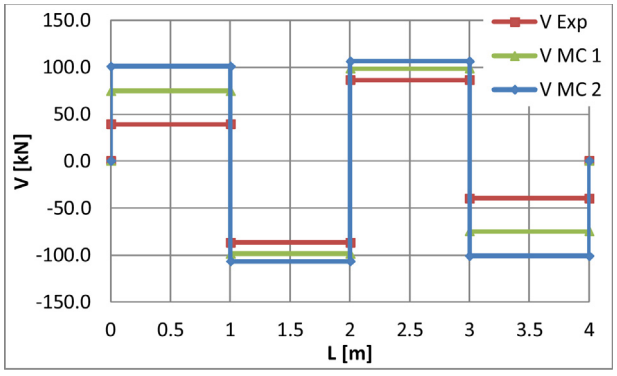

Fig. 16 – Comparison of the shear force value determined experimentally V_{Exp} with the shear capacity calculated according to truss method V_{MC1} and according to SMCFT V_{MC2} - series A-II-S (concrete with steel fibers).

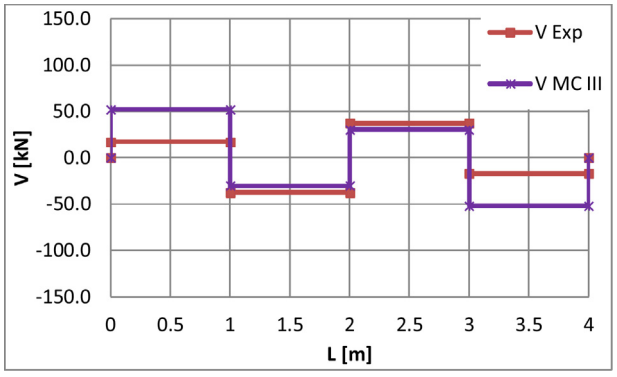

Fig. 18 – Comparison of the shear force value determined experimentally V_{Exp} with the shear capacity calculated on the III level of approximation V_{MCIII} - series A-III-0 (concrete without fibers).

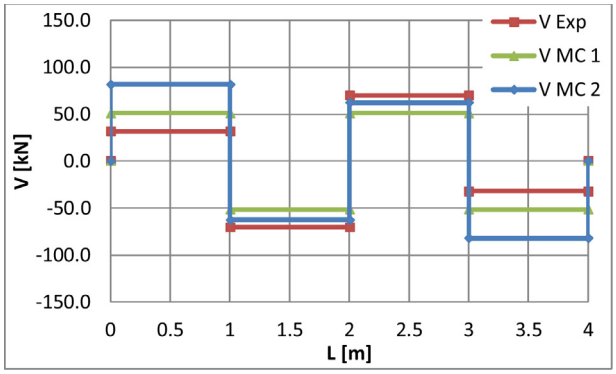

Fig. 19 – Comparison of the shear force value determined experimentally V_{Exp} with the shear capacity calculated according to truss method V_{MC1} and according to SMCFT V_{MC2} - series A-III-S (concrete with steel fibers).

on the shear capacity is taken into account using the ratio of the characteristic residual tensile strength in bending of fiber concrete f_{Ftu}, determined for the opening of the initial crack w_u, to the tensile strength in bending f_{ctk}, in the case of concrete with steel fibers w_u = 1.5 mm, according to the recommendations [26], while in the case of concrete with basalt fibers the maximum w_u value obtained during experimental research [33] is assumed to be equal to 0.8 mm. Load capacity was calculated according to the formula:

$$V_{MC1} = \left\{ \frac{0,18}{\gamma_c} \cdot k \cdot \left[100 \cdot \rho_1 \cdot \left(1 + 7,5 \cdot \frac{f_{Ftuk}}{f_{ctk}} \right) \cdot f_{ck} \right]^{1/3} + 0.15 \cdot \sigma_{cp} \right\} \cdot b_w \cdot d, \tag{4}$$

where: k - factor that takes into account the size effect; d - effective depth of cross section; ρ_1 - reinforcement ratio for longitudinal reinforcement; $\sigma_{cp} = N_{Ed}/A_c < 0.2\ f_{cd}$ - average stress acting on the concrete cross section A_c, for an axial force N_{Ed}, due to loading or prestressing actions.

$V_{MC\ 2}$ – the shear capacity of a fiber concrete element calculated on the basis of the *fib* Model Code procedure [26] based on a simplified modified compression field theory (SMCFT); in the given method, the share of fibers in the transfer of shear stresses was taken into account by introducing the characteristic residual tensile strength of fiber concrete f_{Ftu} determined in the direct tensile test and the corresponding the ultimate crack width w_u and the change in the minimum angle of the compressed strut. Load capacity was calculated according to the formula:

$$V_{MC2} = \frac{1}{\gamma_F} \left(k \cdot \sqrt{f_{ck}} + k_f \cdot f_{Ftuk} \cdot \cot\theta \right) \cdot b_w \cdot z, \tag{5}$$

where: γ_F - partial safety factor for fiber reinforced concrete; k_v - coefficient depending on the longitudinal strain at the mid-depth of the effective shear depth and aggregate size; k_f = 0.8 [26].

Detailed descriptions of the used calculation methods can be found in [26].

The reaction values were determined on the basis of the experimental tests conducted as well as calculated on the basis of the *fib* Model Code guidelines [26]. The values of reactions measured during experimental tests (sum of reactions in Figs. 12–20) agree with the value of the maximum load specified in Table 4. On the other hand, in the case of values calculated according to the *fib* Model Code [26], the formulas proposed in this standard for the shear capacity calculation were used, taking into account the parameters appearing in these formulas.

Figs. 12–20 present a comparison of values of shear forces obtained in the experimental test with the values determined using the calculation procedures discussed above.

The failure of all A-I series beams occurred due to bending, and therefore they did not reach the maximum shear capacity during the test performed. Hence, the calculated values of shear capacity are greater than the shear forces recorded during the test.

The effect of dispersed reinforcement on the shear capacity was taken into account in the calculations of both steel and basalt fiber reinforced concrete beams, by using the characteristic residual tensile strength of f_{Ftu} according to [26]. The shear capacity of the S series beams, calculated for concrete with steel fibers, depending on the calculation method, was greater than the experimentally determined capacity by about 38% (for V_{MC1}) up to 46% (for V_{MC2}) (Fig. 13). As well the presence of basalt fibers in concrete of the B series beams resulted in an increase of the design shear capacity in comparison to the force determined experimentally by 19–38% (Fig. 14).

The destruction of A-II series beams took place first of all as a result of bending and forming of plastic joints, and then - as a result of shear at the central support. Therefore, it is necessary to evaluate the convergence of the results of the experiment and calculations and to analyze the relationship of shear capacity calculated and determined experimentally at the central support, where the beams failed.

In the case of beams without dispersed reinforcement (A-II-0), the calculation procedure [26] on the III level of approximation, allows to exactly determine the values of transverse force (Fig. 15). In this case, full compliance of the values calculated with the results of the experiment was achieved. Beams of A-II-S series failed due to the formation of a plastic hinge at the central support. The calculated values of shear capacity (V_{MC1} andV_{MC2}) were found to be up to 17% greater than the maximum value of the transverse force determined experimentally (Fig. 16).The design shear capacity of beams made of concrete with basalt fiber (Fig. 17), depending on the method,

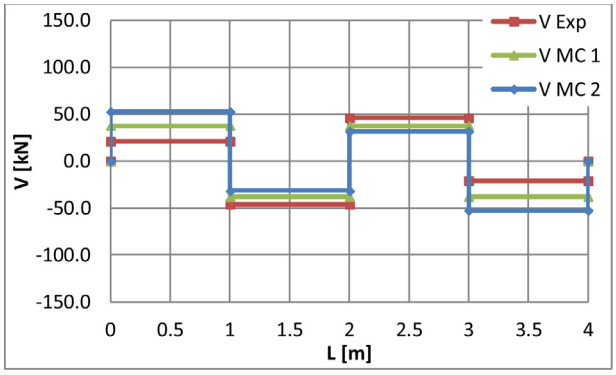

Fig. 20 – Comparison of the shear force value determined experimentally V_{Exp} with the shear capacity calculated according to truss method V_{MC1} and according to SMCFT V_{MC2} - series A-III-B (concrete with basalt fibers).

was higher by 8% (V_{MC2}) or less by 12% (V_{MC1}) in comparison to the value of capacity obtained during the test.

For all A-III series of beams, the failure occurred at the center support as a result of shearing. Thus, in this case the calculated and experimental shear capacity of beams determined at the center support were compared. The values of the calculated capacities, regardless of the calculation method used, were smaller than those obtained during the experiment. In the A-III-S series (Fig. 19) the difference between the value of the load determined experimentally and calculated according to the truss method (V_{MC1}) was 17%. This means that the estimated design values of the ultimate force give a small reserve of capacity, and at the same time allow to determining the value of this force with a sufficient approximation. However, based on the analysis of fiber concrete beams of the A-III-B series (Fig. 20), it was found that the results obtained using the V_{MC1} calculation method more accurately reflect the experimental results than the V_{MC2} calculation (the differences were 16% and 31%, respectively).

5. Conclusions

Based on the experimental study, the following conclusions can be drawn:

1 The presence of both steel and basalt fibers in concrete affects the change of the failure mode of beams under bending to a more ductile character. Steel fibers were more effective in reducing the cracking and deformations of concrete beams.
2 The beneficial influence of incorporating basalt or steel fibers in concrete on the load capacity of two-span beams can be observed on the basis of the ultimate force values recorded during test.
3 The incorporation of steel fibers at the content of 78.5 kg/m^3 (1.00% by volume) into concrete causedup to 30% increase in the value of load initiating the diagonal crack formation. In the case of basalt fibers added at the content of 5 kg/m^3 (0.19% by volume) the value of this load increased about 15%.
4 Both types of fibers can be considered as an alternative shear reinforcement replacing, at least partially, steel stirrups. However, in comparison to concrete beams without fibers, the beneficial effect of basalt fibers has been revealed in the series with 50% reduced stirrup reinforcement.
5 Digital Image Correlation (DIC) analysis of crack pattern around the central support confirmed the influence of both sorts of fibers on crack pattern and shear behavior of beams with reduced reinforcement for shear.
6 The methods of calculating the shear capacity of beams made of concrete with fibers and without fibers proposed in *fib* Model Code have been verified and the results were found satisfactory. The calculations adequately reflect the results of experimental tests in cross-sections in which beams reached their shear capacity.

Author agreement/declaration

All authors have seen and approved the final version of the manuscript being submitted.

Conflict of interest

None declared.

Ethical statement

Authors state that the research was conducted according to ethical standards.

Funding source declaration

This research work was financially supported by National Centre for Research and Development, Poland; project number PBS3/A2/20/2015 (ID 245084).

REFERENCES

[1] A. Picazo, J.C. Galvez, M.G. Alberti, A. Enfedaque, Assessment of the shear behaviour of polyolefin fibre reinforced concrete and verification by means of digital image correlation, Constr. Build. Mater. 181 (2018) 565–578.
[2] A. Brandt, Fibre reinforced cement-based (FRC) composites after over 40 years of development in building and civil engineering, Compos. Struct. 86 (1-3) (2008) 3–9.
[3] P. Serna, S. Arango, T. Ribeiro, A.M. Núñez, E. Garcia-Taengua, Structural castin-place SFRC: technology, control criteria and recent applications in Spain, Mater. Struct. 42 (9) (2009) 1233–1246.
[4] J.A. Lopez, P. Serna, E. Camacho, H. Coll, J. Navarro-Gregori, First ultra-high performance fibre-reinforced concrete footbridge in Spain: design andconstruction, Struct. Eng. Int. 24 (1) (2014) 101–104.
[5] G. Tiberti, F. Minelli, G. Plizzari, Reinforcement optimization of fiber reinforced concrete linings for conventional tunnels, Compos. Part B: Eng. 58 (2014) 199–207.
[6] S.P. Shah, B.V. Rangan, Fiber reinforced concrete properties, ACI J. Proc. 68 (2) (1971) 126–135.
[7] Q. Chunxiang, I. Patnaikuni, Properties of high-strength steel fiber-reinforced concrete in bending, Cem. Concr. Compos. 21 (1999) 73–81.
[8] H.H. Dinh, G.J. Parra-Montesinos, J.K. Wight, Shear behavior of steel fibre-reinforced concrete beams without stirrup reinforcement, ACI Struct. J. 107 (2010) 597–606.
[9] J. Susetyo, P. Gauvreau, F.J. Vecchio, Effectiveness of steel fiber as minimum shear reinforcement, ACI Struct. J. 108 (2011) 488–496.
[10] F. Minelli, G.A. Plizzari, On the effectiveness of steel fibers as shear reinforcement, ACI Struct. J. 3 (2013) 379–389.
[11] F.A. Farhat, D. Nicolaides, A. Kanellopoulos, B.L. Karihaloo, High performance fibre-reinforced cementitious composite (CARDIFRC) - Performance and application to retrofitting, Eng. Fract. Mech. 74 (2007) 151–167.
[12] P. Soroushian, C.D. Lee, Distribution and orientation of fibers in steel fiber reinforced concrete, ACI Mater. J. 87 (5) (1990) 433–439.
[13] M.G. Alberti, A. Enfedaque, J.C. Gálvez, On the prediction of the orientation factor and fibre distribution of steel and macro-synthetic fibres for fibre reinforced concrete, Cem. Concr. Compos. 77 (2017) 29–48.
[14] T.M. Borhan, Properties of glass concrete reinforced with short basalt fibre, Mater. Des. 42 (2012) 265–271.

[15] J. Branston, S. Das, S.Y. Kenno, C. Taylor, Mechanical behaviour of basalt fibre reinforced concrete, Constr. Build. Mater. 124 (2016) 878–886.
[16] M. Imam, L. Vandewalle, F. Mortelmans, D. Van Gemert, Shear domain of fiber-reinforced high-strength concrete beams, Eng. Struct. 9 (1997) 738–747.
[17] S. Altoubat, A. Yazdanbakhsh, K. Rieder, Shear behavior of macro-synthetic fiber-reinforced concrete beams without stirrups, ACI Mater. J. 106 (2009) 380–389.
[18] Y.L. Voo, W.K. Poon, S.J. Foster, Shear strength of steel fiber-reinforced ultra high-performance concrete beams without stirrups, J. Struct. Eng. 136 (11) (2010) 1393–1400.
[19] A. Meda, F. Minelli, G.A. Plizzari, P. Riva, Shear behaviour of steel fibrereinforced concrete beams, Mater. Struct. 38 (3) (2005) 343–351.
[20] M.F. Ruiz, A. Muttoni, J. Sagaseta, Shear strength of concrete members withouttransverse reinforcement: a mechanical approach to consistently account for sizeand strain effects, Eng. Struct. 99 (2015) 360–372.
[21] J.S. Lawler, T. Wilhelm, D. Zampini, S.P. Shah, Fracture processes of hybrid fiber-reinforced mortar, Mater. Struct. 36 (2003) 197–208.
[22] A. Jansson, M. Flansbjer, I. Lofgren, K. Lundgren, K. Gylltoft, Experimental investigation of surface crack initiation, propagation and tension stiffening in self-compacting steel-fibre-reinforced concrete, Mater. Struct. 45 (8) (2012) 1127–1143.
[23] E. Bentz, F. Vecchio, M. Collins, Simplified modified compression field theory for calculating shear strength of reinforced concrete elements, ACI Struct. J. 103 (S65) (2006) 614–624.
[24] Z.P. Bažant, Q. Yu, W. Gerstle, J. Hanson, J.W. Ju, Justification of ACI 446 proposal forupdating ACI code provisions for shear design of reinforced concrete beams, ACI Struct. J. 104 (5) (2007) 601–610.
[25] A. Cladera, A. Marí, C. Ribas, J. Bairán, E. Oller, Predicting the shear–flexural strength of slender reinforced concrete T and I shaped beams, Eng. Struct. 101 (2015) 386–398.
[26] Model Code 2010, Comité Euro-International du Béton fib (CEB-FIP), 2012.
[27] V. Sigrist, E. Bentz, M.F. Ruiz, S. Foster, A. Muttoni, Background to the fib Model Code 2010 shear provisions - part 1: beams and slabs, Struct. Concr. 14 (3) (2013) 195–203.
[28] EN 1992-1-1 Eurocode 2 - Designing concrete structures - Part 1-1: General rules and rules for buildings.
[29] T. Mészöly, N. Randl, Shear behavior of fiber-reinforced ultra-high performance concrete beams, Eng. Struct. 168 (2018) 119–127.
[30] C. High, H.M. Seliem, A. El-Safty, S.H. Rizkalla, Use of basalt fibers for concrete structures, Constr. Build. Mater. 96 (2015) 37–46.
[31] B. Wei, H. Cao, S. Song, Environmental resistance and mechanical performance of basalt and glass fibers, Mater. Sci. Eng. A 527 (2010) 4708–4715.
[32] J. Sim, C. Park, D.Y. Moon, Characteristics of basalt fibre as a strengthening material for concrete structures, Compos. Part B Eng. 36 (2005) 504–512.
[33] M. Kosior-Kazberuk, J. Krassowska, Post-cracking behaviour of basalt fibre reinforced concrete, in: Proc. 6th International Conference on Mechanics and Materials in Design: M2D2015, 2015.
[34] J. Krassowska, M. Kosior-Kazberuk, Failure mode in shear of steel fiber reinforced concrete beams, in: Proc. 8th Scientific-Technical Conference on Material Problems in Civil Engineering: MATBUD'2018, 2018.
[35] EN 12390-3 Concrete tests - Part 3: Compressive strength of test specimens.
[36] EN 12390-5 Concrete testing - Part 5: Bending strength of test specimens.
[37] EN 12390-13 Concrete tests - Part 13: Determination of the secant elastic modulus under compression.
[38] EN 12390-6 Concrete tests - Part 6: Tensile splitting strength of test specimens.
[39] S.Y. Alam, A. Loukili, F. Grondin, E. Roziere, Use of digital correlation and acoustic emission technique to study the effect of structural size on cracking of reinforced concrete, Eng. Fract. Mech. 143 (2015) 17–31.
[40] M. Hamrat, B. Boulekbache, M. Chemrouk, S. Amziane, Flexural cracking behavior of normal strength, high strength and high strength fiber concrete beams, using Digital Image Correlation technique, Constr. Build. Mater. 106 (2016) 678–692.